

7 Supplementary material for LHCb-PAPER-2014-029

This appendix contains supplementary material that will be posted on the public cds record but will not appear in the paper.

Stability of the $\eta_c(1S)$ to J/ψ production ratio under variation of the t_z requirement is checked by applying an alternative requirement at 120 fs. The yield ratios $N_{\eta_c(1S)}^P/N_{J/\psi}^P$ for prompt production are determined to be 1.21 ± 0.22 using the $\sqrt{s} = 7$ TeV data sample, and 1.08 ± 0.21 using the $\sqrt{s} = 8$ TeV data sample. The yield ratios $N_{\eta_c(1S)}^S/N_{J/\psi}^S$ for charmonium production from b -hadron decays are determined to be 0.30 ± 0.06 using the $\sqrt{s} = 7$ TeV data sample, and 0.31 ± 0.04 using the $\sqrt{s} = 8$ TeV data sample. The differences between these values and the nominal ones, corresponding to the 80 fs requirement, are small compared to their statistical uncertainty. Figures 4 and 5 show distributions of the t_z variable for simulated charmonium signal selected in the prompt sample and in the sample from b -hadron decays, respectively. The simulation sample corresponds to about 15% of the LHCb collected data. The turn on of the t_z distribution around 0.25 ps is caused by the selection criterion on high impact parameter significance, $\chi_{\text{IP}}^2/\text{ndf} > 16$, which selects preferentially proton-proton pairs displaced from the primary vertex.

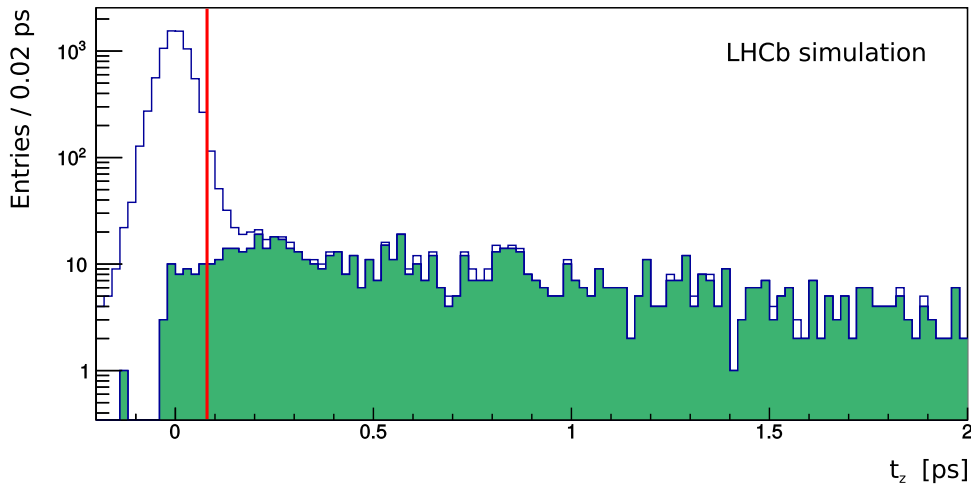


Figure 4: Distribution of the pseudo-decay time t_z for simulated $J/\psi \rightarrow p\bar{p}$ signal selected by the prompt production analysis. All selection criteria but the t_z requirement are applied. The t_z threshold is shown with the red vertical line. Empty and filled histograms correspond to prompt charmonia and charmonia from b -hadron decays, respectively.

The cross-sections for $\eta_c(1S)$ prompt production at $\sqrt{s} = 7$ TeV and $\sqrt{s} = 8$ TeV centre-of-mass energies in the LHCb acceptance (rapidity range $2.0 < y < 4.5$) for $p_T > 6.5$ GeV/ c , are shown on Fig. 6 and 7 with statistical and systematic uncertainties, and the uncertainty associated with the $J/\psi \rightarrow p\bar{p}$ and $\eta_c(1S) \rightarrow p\bar{p}$ branching fractions and the J/ψ cross-section measurement, shown separately.

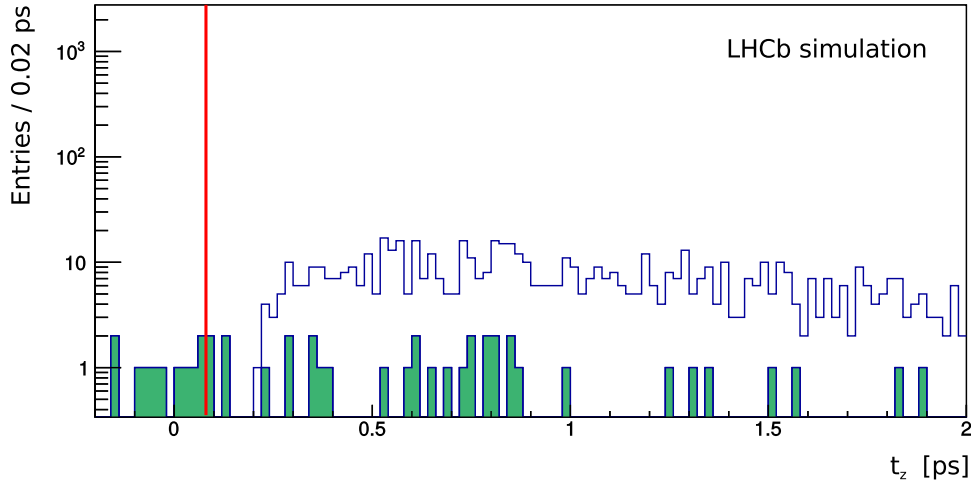


Figure 5: Distribution of the pseudo-decay time t_z for simulated $J/\psi \rightarrow p\bar{p}$ signal selected by the analysis of charmonia production in b -hadron decays. All selection criteria but the t_z requirement are applied. The t_z threshold is shown with the red vertical line. Empty and filled histograms correspond to charmonia from b -hadron decays and prompt charmonia, respectively.

332 Figure 8 shows a contour plot for the η_c natural width $\Gamma_{\eta_c(1S)}$ and the mass difference
 333 $\Delta M_{J/\psi, \eta_c(1S)}$, using the combined data sample. The 2011 and 2012 results are consistent.

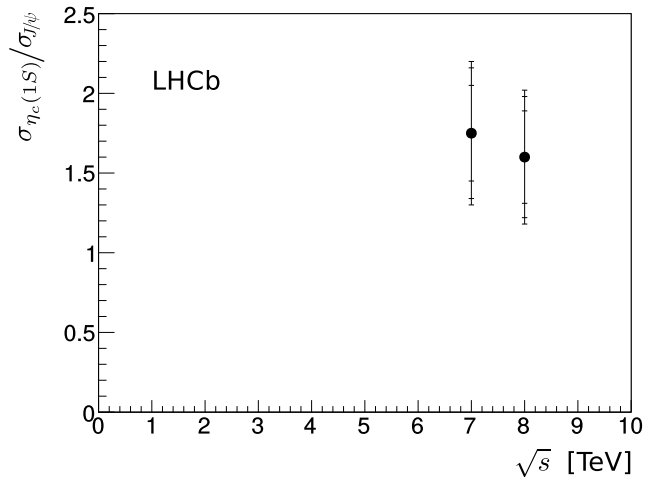


Figure 6: Relative $\eta_c(1S)$ to J/ψ prompt production cross-section as a function of collision energy. Inner error bars on the plot correspond to statistical uncertainty, middle error bars correspond to the quadratic sum of statistical and systematic uncertainties, and outer error bars correspond to the quadratic sum of statistical and systematic uncertainties and the uncertainty associated to the $J/\psi \rightarrow p\bar{p}$ and $\eta_c(1S) \rightarrow p\bar{p}$ branching fractions. The systematic uncertainty and the uncertainty associated to the branching fractions are correlated between the measurements at $\sqrt{s} = 7$ TeV and $\sqrt{s} = 8$ TeV.

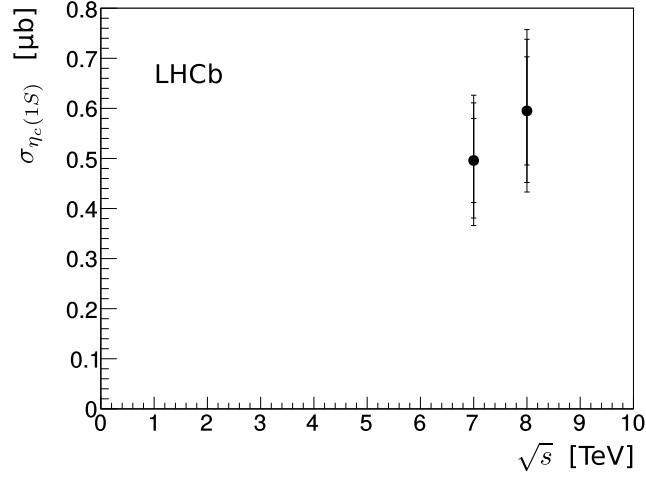


Figure 7: Cross-section of the $\eta_c(1S)$ prompt production as a function of collision energy. Inner error bars on the plot correspond to statistical uncertainty, middle error bars correspond to the quadratic sum of statistical and systematic uncertainties, and outer error bars correspond to the quadratic sum of statistical and systematic uncertainties and the uncertainty associated to the $J/\psi \rightarrow p\bar{p}$ and $\eta_c(1S) \rightarrow p\bar{p}$ branching fractions. The systematic uncertainty and the uncertainty associated to the branching fractions are correlated between the measurements at $\sqrt{s} = 7$ TeV and $\sqrt{s} = 8$ TeV.

334 The combined result and the individual 2011 and 2012 results are consistent with the
 335 world average values [21].

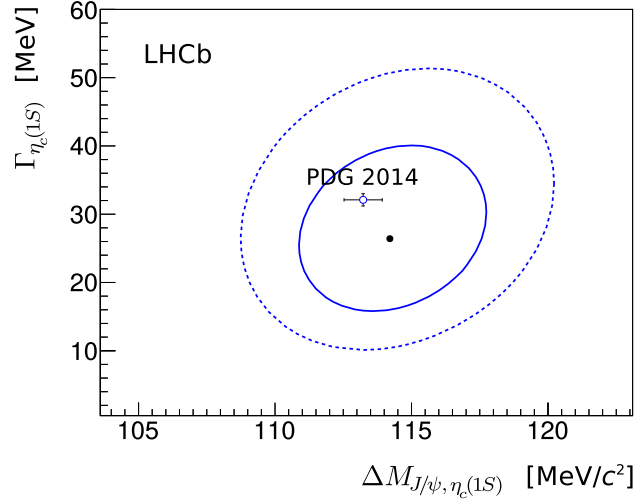


Figure 8: Contour plot of $\Gamma_{\eta_c(1S)}$ and $\Delta M_{J/\psi, \eta_c(1S)}$ for the combined data sample. The curves indicate 68.3 C.L. (one-sigma) and 95.5 C.L. (two-sigma) contours. Only statistical uncertainties are shown. The world-average [21] value is indicated as an empty circle with error bars.